J. Micromech. Microeng. **19** (2009) 105007 (11pp) doi:10.1088/0960-1317/19/10/105007

An endoscopic capsule robot: a meso-scale engineering case study

Claudio Quaglia[1], Elisa Buselli[1], Robert J Webster III[2], Pietro Valdastri[1], Arianna Menciassi[1,3] and Paolo Dario[1,3]

[1] Scuola Superiore Sant'Anna—CRIM Lab, Viale R Piaggio 34, Pisa, Italy
[2] Department of Mechanical Engineering, Vanderbilt University, 2301 Vanderbilt Place, Nashville, TN, USA
[3] Italian Institute of Technology Network, Genova, Italy

E-mail: pietro@sssup.it

Received 10 August 2009
Published 16 September 2009
Online at stacks.iop.org/JMM/19/105007

Abstract

A number of unique challenges arise in fabricating and assembling complex mechanisms at the meso-scale (hundreds of microns to centimetres). In general, for a complex multi-part mechanism at this length scale, no single machining technique can produce all the necessary parts—or often even a single individual part. Towards developing a comprehensive set of 'best practices' for combining multiple precision micromachining operations at the meso-scale, we present a case study on fabricating and assembling an endoscopic capsule robot. Existing passive imaging capsules have proven exceptionally useful in the diagnosis of the gastrointestinal tract, and robotic capsules promise to enhance their diagnostic capabilities and enable non-invasive treatment delivery. In this case study, we describe the fabrication of a robotic capsule (2.6 cm^3 in volume) containing a complex mechanism consisting of 72 components, each of which requires a variety of meso- or even micro-scale features. We describe the manufacturing processes used to produce these components and features (combinations of high precision, multiply refixtured computer numerical control processes, sink and wire electro discharge machining , laser cutting, etc). These results contribute to the emerging framework of best practices in meso-scale design and manufacture, illustrating ways to effectively combine several processes to produce a complex meso-scale device.

(Some figures in this article are in colour only in the electronic version)

1. Introduction

The meso-scale can be defined as the dimensions that lie between the traditional macro and micro-scales, from hundreds of microns to centimetres [1, 2]. This length scale presents a number of unique design and fabrication challenges. Components often must be fabricated in a multi-step process requiring refixturing between steps and/or combinations of several different manufacturing technologies to create a single part. Assemblies made from such components must be carefully designed with appropriate tolerances between their reference surfaces. Strategies must also be developed for maintaining manufacturing accuracy when refixturing or moving parts between machines. Developing a general framework of best practices for such meso-scale design, fabrication and assembly tasks can be facilitated by case studies such as the endoscopic capsule robot that we discuss in this paper. Such case studies serve to elucidate the challenges and possible solutions involved in creating complex assemblies at the meso-scale.

In this paper, we present the design, fabrication and assembly of a novel wireless endoscopic capsule robot intended for medical applications (see figures 1–3). Capsule robots must be small enough to swallow and require complex miniature mechanisms in order to control their position and orientation. The prototype we discuss in this paper matches the dimensions of commercial, Food and Drug Administration (FDA) approved 'camera pills' [3] almost exactly. It is a cylinder 11.1 mm in diameter and 27 mm long and it contains 72 components. Fabricating these components required the combination of a number of manufacturing techniques including computer numerical control (CNC),

Figure 1. The assembled endoscopic capsule robot that is the focus of our case study. Its internal components are shown in figure 3.

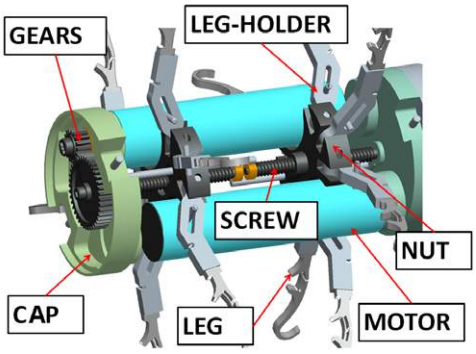

Figure 2. CAD drawing of the assembled internal components of the capsule robot. Component dimensions range from 23.6 mm (length of the capsule body) to 0.4 mm (diameter of the pins).

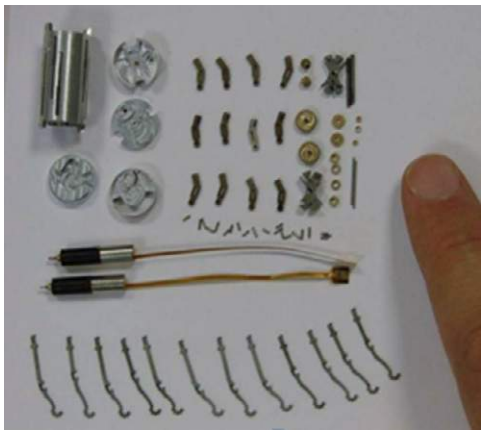

Figure 3. Fabricated internal mechanical components of the capsule robot before assembly. The assembly procedure is discussed in section 5, and the assembled prototype is shown in figure 1.

sink and wire electro discharge machining (EDM) and laser cutting.

The paper is organized as follows: section 2 presents related work in meso-scale design and fabrication, as well as the background and medical motivation for capsule robots. In section 3, we discuss individual components themselves, material choices and fabrication procedures. Then, in section 4 we present experimental assessment of fabrication accuracy of individual components. In section 5, we discuss the assembly procedure for the capsule robot. Section 6 summarizes and discusses results, highlighting the lessons learned from this case study for future meso-scale design and manufacturing tasks.

2. Background and related work

2.1. Background on meso-scale fabrication

Meso-scale components with complex features are increasingly required in aerospace, electronics, biomedicine and communications, among other applications. A survey of currently available techniques for the meso-scale reveals two main approaches: scaling up technologies typically applied in microelectromechanical systems (MEMS) or scaling down macro-scale techniques using ultra-precision machining [4]. MEMS techniques are generally used for micro-fabrication and are limited to thick 2D structures and a narrow class of (mainly silicon-based and thus fragile) materials [5].

Ultra-precision machines can overcome these problems, since they can machine 3D geometry using many types of materials. However, they do not allow batch fabrication, thus requiring considerable time to reproduce large numbers of small features or to make multiple copies of a given part. Some recent innovative approaches, such as shape deposition manufacturing (SDM), may eventually overcome this. While still in early stages of development, SDM has the potential to create moulds with complex shapes for forming multi-material meso-scale devices [6, 7].

Another challenge associated with scaling down large-scale machining techniques is obtaining sufficiently high accuracy for miniaturized components. This is not straightforward, due to the lack of small and precise tools and the inertia of the machine tool, which can lead to substantial errors at the meso-scale. Other effects that may be neglected at the macro-scale can also become critical at the meso-scale (e.g. lattice microstructure and surface effects). In order to overcome the limitations of current technologies, many researchers are developing new machines and tools specifically designed for meso-scale products [8–10], aiming towards the design of microfactories integrating these machines [11], eventually assisted by robotic technologies [12]. A survey of the current efforts in mechanical micro-machining research and applications is available in [13].

Until such technologies achieve their promise and reach maturity, the best available options for precise fabrication at the meso-scale are the use of advanced, but still in principle traditional, ultra-precision machines. Thus, in this work, we present a centimetre-scale robot with most components in the meso-scale domain and several features in the micro-scale, completely developed by ultra-precision machines. A review of the state of the art in ultra-precision machining is available in [14]. A discussion on the limits of EDM technology and a description of a new method to machine complex micro-cavities are available in [15]. It is also possible to use this approach in tandem with the computer-aided design (CAD) software to produce small features with exceedingly high precision [16], by compensating for electrode wear during

the machining process. Our interest in the present paper is not to probe the fundamental limits of such manufacturing technologies, but rather to investigate means of combining ultra-precision machining techniques to produce a complex meso-scale mechanism.

2.2. Medical motivation for capsule robots

Encapsulating a camera within a pill is a recent innovation in medical technology [17] which enables non-invasive visual diagnosis deep within the intestine. The images returned by these wireless capsule endoscopes (WCEs) are extremely valuable medically. They can reveal the location and severity of lesions or bleeding, enable inspection of potentially cancerous growths in the intestinal wall, permit visual assessment of the overall health of the gastrointestinal (GI) tract, etc. An expanded discussion of the clinical value of WCEs can be found in [18].

Despite these revolutionary capabilities, current WCEs are unable to directly control their position and orientation within the GI tract and must rely on peristalsis—muscle contractions that ordinarily move food during digestion—to propel themselves. This means that they cannot adjust their speed, stop or reverse direction, which limits both the quantity and quality of images returned from the site of interest. Such limitations are particularly problematic in the large intestine where WCEs tumble unpredictably due to the large difference between capsule diameter and intestine diameter.

A possible solution consists in a miniature propulsion system integrated within the WCE [19]. In particular, an approach that is particularly well suited to the challenging environment of the GI tract is of legged locomotion [20]. In prior work, the authors have presented a series of increasingly advanced prototype capsules for robotic legged locomotion [21, 22].

The most advanced of these legged capsule robots to date is the 12-leg prototype, for which the design methodology, medical considerations and control strategies can be found in [23]. In following sections, we describe the fabrication of this robot as a case study on meso-scale component design and fabrication.

2.3. Capsule robot case-study overview

The capsule robot shown in figure 1 contains two motors (Namiki Precision Jewel Co. Ltd), each of which independently controls a set of six legs. As shown in figure 2, each motor is coupled to a lead screw through a gear transmission. As the lead screw rotates, a nut connected by pins to leg holders translates axially with respect to the capsule. The leg holders are also connected via a slotted pin connection to the capsule exterior wall. Thus, the leg set opens and closes in an 'umbrella-like' manner as the nut translates. As can be seen in figures 2 and 3, there are a large number of meso- and even micro-scale features on the components in this mechanism, and thus its fabrication is an illuminating case-study in meso-scale engineering.

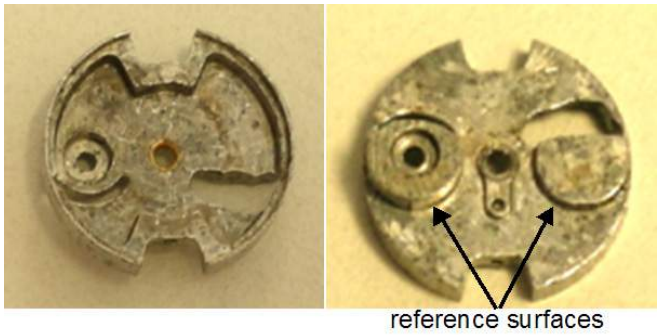

Figure 4. The two faces of one of the caps. The two cylindrical protrusions, that are the reference surfaces, are 3.85 mm in diameter and the inter-axis spacing is 6.8 mm.

3. Fabricating capsule robot components

In this section, we describe the manufacturing procedures for the components shown in figure 3. We begin with the capsule cap and body that provide the outer casing for the capsule and then proceed inward along the kinematic chain from the leg to the leg holder to the lead screw to the gears that couple lead screws to motor shafts. In addition to a brief description of each component, we describe each fabrication strategy employed and the rationale behind it. Most of the 72 components were fabricated using one or more of these machines:

(1) Lathe (17D, EMCOMAT, Germany);
(2) CNC 5 axis milling machine (HSPC, KERN, Germany);
(3) Sink EDM (T1-T4 SR-HPM, Sarix, Switzerland);
(4) Wire EDM (AP 200 L, Sodick, Japan);
(5) Laser machining: (Nd-YAG laser, Trumpf, Germany).

3.1. The cap

3.1.1. Description. There are four caps, two for each end of the capsule. Each has a diameter of 11.1 mm and was machined to house bushings, gears and electronics (see figure 4). The caps also contain two reference surfaces each, to allow repeatable connection between caps and the capsule body. These features are highlighted in figure 4.

The caps and body were machined in Ergal 7075 using the HSPC KERN milling machine. Ergal has a unique blend of machinability, wear resistance and lightness that make it a popular material choice in airplane manufacture.

3.1.2. Fabrication strategy. The cap was machined starting from a rod workpiece. It was fixtured on the HSPC KERN chuck and both the internal and external surfaces and all the holes and reference surfaces were machined on one side. The workpiece was then cut to the proper length using a lathe. It was then inverted and refixtured on the HSPC KERN for machining of the opposite side (see figure 4 for the two finished faces, and figure 5 for refixturing images). In order to perform this step maintaining correct reference to the side which was already shaped, a custom cap fixture was fabricated directly on the HSPC KERN. It was built using a cylindrical

Figure 5. The custom cap fixture used for refixturing the caps on the machine. The holes shown are 3.95 mm in diameter. The right image shows the fixture with a cap in place on it, just after machining the cap's second face.

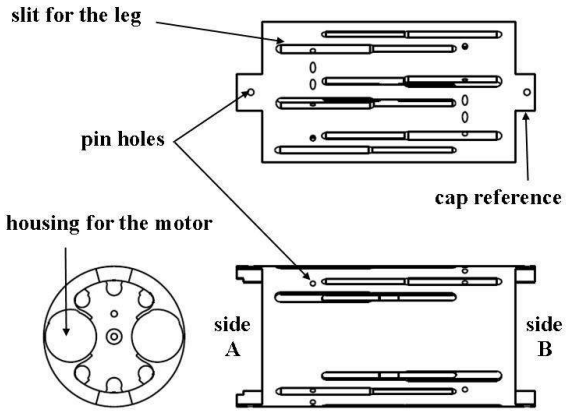

Figure 6. The capsule body is 11.1 mm in diameter, 23.6 mm long and its smallest features are 12 holes of 0.4 mm diameter.

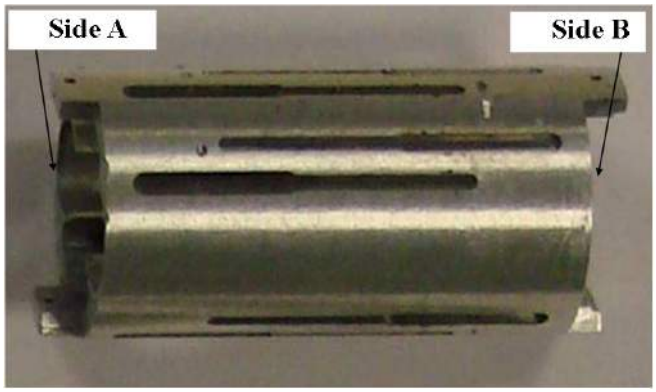

Figure 7. The fabricated capsule body, made from Ergal.

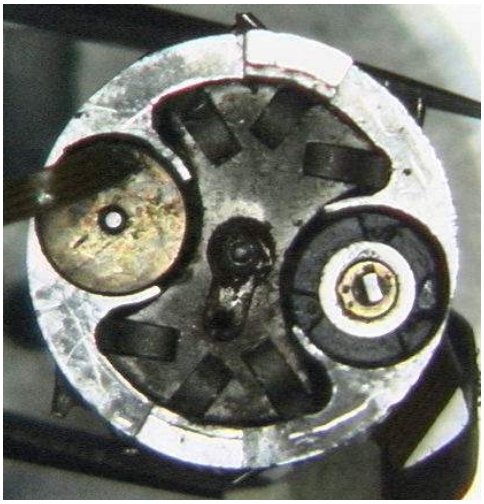

Figure 8. An axial view of the capsule, showing assembled motors (right and left circular parts) and the central nut.

workpiece, into which was machined a negative cap profile (figure 5). After machining, this cap fixture was left in place on the HSPC KERN, to remove chuck jaw refixturing as a source of error. The cap was then bonded to the cap fixture using cyanoacrylate glue and the second face of the cap was machined. To disassemble the cap from the cap fixture after removal from the HSPC KERN, both the parts were dipped into an acetone solvent to release the glue.

The critical dimensions of the cap fixture were the two holes that guarantee a precise assembly with the cap. The distances between the hole centres in the fixture were designed to be slightly bigger than in the cap, in order to obtain an easy and accurate placement. Therefore, we chose a tolerance of -0.03 mm for this parameter. Given this assumption, the interference with the cap should not exceed 0.06 mm. See section 4.1 for further details on these dimensions.

An additional challenge in cap fabrication was machining the several thin regions (approximately 150 μm) they contained. Through a trial and error procedure performed with the HSPC KERN, it was determined that these thin regions could be fabricated without significant material deformation provided that the tool feed was reduced approximately 30% from the tool supplier recommendations for Ergal.

3.2. The body

3.2.1. Description. The capsule body has a diameter of 11.1 mm and a length of 23.6 mm and houses all internal components. Twelve 14.1 mm slits for the legs are cut into its external surface, along with 0.4 mm diameter holes for each of the pins that support the leg holders at the capsule wall (see figure 6).

3.2.2. Fabrication strategy. Creating the internal features of the capsule body (figures 7 and 8) required two processes—one from each end of the cylinder—for two reasons. First, small internal features require use of a small-diameter end mill, which must have a correspondingly short cutting length to prevent tool chatter. Second, the internal geometry does not go all the way through the capsule—a 'plate' of material 1.5 mm thick is left in the middle of the capsule body to support the bushings which hold the ends of the lead screws.

Thus, the capsule body began as a solid cylindrical Ergal workpiece 11.1 mm in diameter, which was machined on one end (side A shown in figure 7) using the HSPC KERN to create the profile shown in figure 8. Then the workpiece was cut to length using a lathe in preparation for machining side B. In

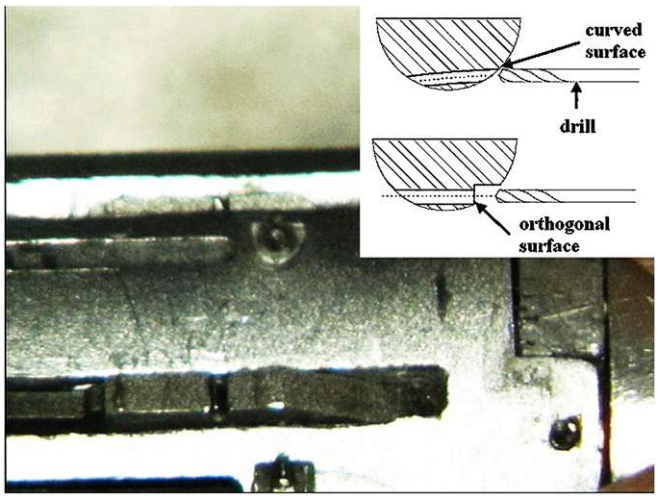

Figure 9. The levelled surface for the hole. Inserted into the hole is a pin within a bushing. The inset line drawing shows the trajectory of a drill bit on rounded versus levelled surfaces.

order to accurately refixture the workpiece, using the same strategy as described above with respect to cap manufacture, a custom body fixture (a negative of the profile shown in figure 8) was machined separately. As with the caps, side A was then attached to this fixture (again, without removing the fixture from the machine) to enable accurate manufacture of side B. This procedure enabled accurate references to be maintained for the refixtured part and ensured that profiles on sides A and B were aligned both axially and radially.

Next, without refixturing (taking advantage of the 5 axes of the machine), the leg slots were machined into the wall of the cylinder, and finally the holes for the capsule-wall pins (which support the leg-holders) were drilled. Drilling these holes was challenging due to the curved surface of the capsule body. This required first levelling the surface with a small end mill and then drilling the hole (figure 9), to prevent drill bit deflection.

3.3. The leg

3.3.1. Description. The legs are the distal elements of the kinematic chain that begins at the motors within the capsule body. The 'feet' at leg tips interface the colon walls and enable locomotion as the leg makes a 'stride'. In order to adapt foot position and leg shape to a variety of diameters commonly found in the intestine and prevent injury to the tissue, the leg were fabricated from Nitinol, a nickel–titanium alloy. When appropriately heat treated, Nitinol exhibits superelastic properties (approximately 8% recoverable strain) at both room and body temperature. Elasticity, combined with flexure joints, creates a leg that is both gentle to tissue and provides sufficient friction and normal force for capsule propulsion. Further information and experimental results on capsule leg design can be found in [24]. The legs used in this study were 9.4 mm in length and 0.5 mm thick (see figure 10).

3.3.2. Fabrication strategy. The leg was cut from a Nitinol sheet (alloy S—superelastic standard alloy, Memory-Metalle GmbH, Germany) using wire EDM. A number of leg designs

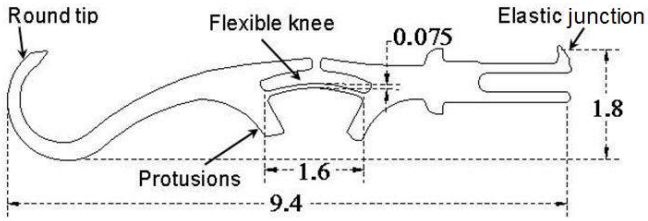

Figure 10. An example schematic drawing of a capsule robot leg. All dimensions are in mm.

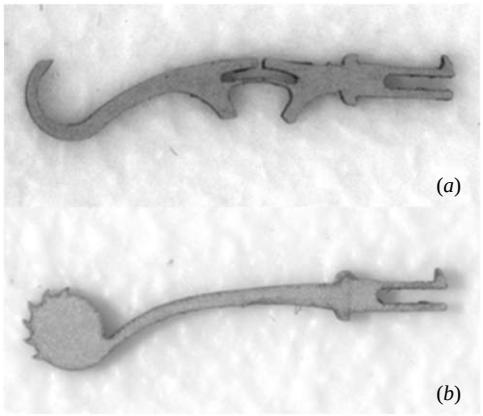

Figure 11. Two example of leg designs for the capsule robot.

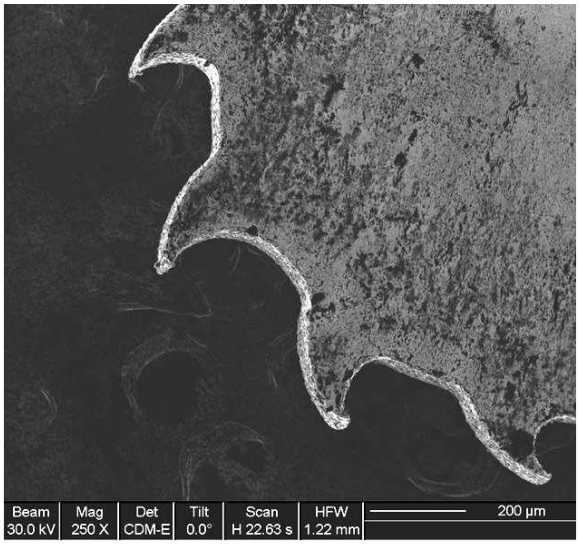

Figure 12. A focused ion beam (FIB) image of micro-hooks at leg tips on leg (*b*) in figure 11.

were machined, and two are shown in figure 11. In one design (figures 10 and 11(*a*)) the leg includes a flexible 'knee' joint 0.075 mm wide that provides a passive degree of freedom, reaching a maximum angle of 75°. A second type of leg (figure 11(*b*)) includes a 'foot' equipped with micro-hooks (about 100 μm long) to enhance superficial friction with the tissue (figure 12).

A primary technical challenge in leg manufacture was shaping the knee accurately. Leg flexibility is proportional to the third power of width, so small inaccuracies in fabrication can have a significant effect on final stiffness. This problem

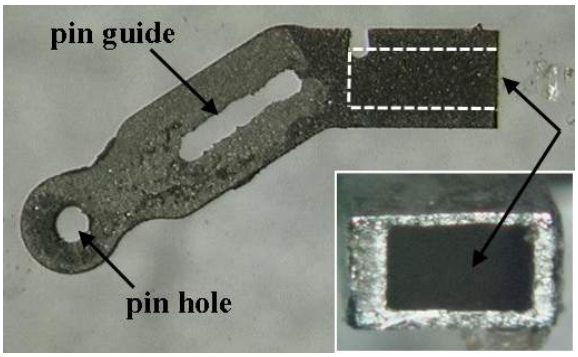

Figure 13. A longitudinal section of the leg holder. Its total length is 7.38 mm, while its minimum feature, the pin guide, is 0.4 mm wide. The inset shows the leg seats.

was addressed by using an initial rough cut, followed by several finishing passes to cut the knee to the desired dimensions.

Laser cutting was also investigated as an alternative fabrication technique, given its higher speed if compared to wire EDM. Thus legs in the shapes represented in figures 10 and 11(*a*) were also cut using the laser cutter mentioned previously.

3.4. The leg holder

3.4.1. Description. Working inward along the kinematic chain, each leg snaps into a leg-holder (figure 13), which interfaces with a pin at the capsule wall and a pin on the nut threaded onto the lead screw (see figure 2). The leg holder was fabricated from steel (all components in the capsule that are subject to high mechanical stresses or friction were machined in steel to reduce wear and prolong the life of the capsule).

3.4.2. Fabrication strategy. The external profile of the leg holder was machined using wire EDM and the pockets into which the legs snap (the 'leg seats') were fabricated using sink EDM. For this purpose, an electrode that was a negative of the leg seat was fabricated both using the HSPC KERN (rough shaping to enable fixturing of the part in the sink EDM machine) and wire EDM (for cutting the electrode profile). The resulting negative electrodes are shown in figure 14. The negative electrode has the dimensions of the leg seat pocket: a rectangular profile 0.9 mm wide and 0.5 mm thick. Unfortunately, the electrical arcs used in plunge etching do gradually wear away the electrode material. For this reason, we fabricated several electrode negatives for the leg seats, as shown in figure 14. In particular, three electrodes were required to machine each leg holder.

The pin guide (see figure 13) was machined by wire EDM starting from a smaller diameter hole made with a standard drill. In order to achieve high surface quality with the wire EDM, we refined the shape through several finishing passes after an initial rough cut.

3.5. The lead screw

3.5.1. Description. Two steel lead screws were used to drive the nuts that impart force to the leg holders. On one end

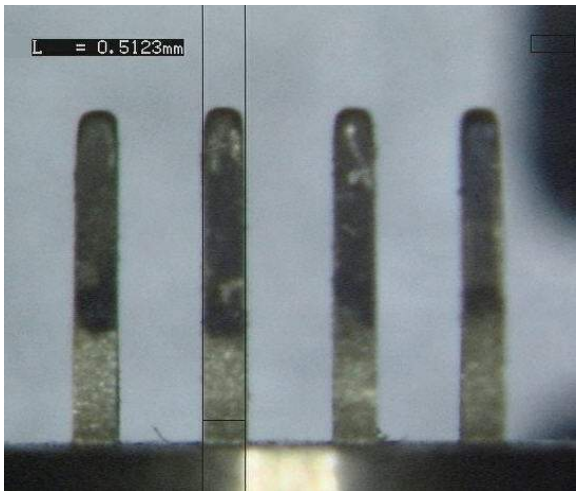

Figure 14. A photo taken after using the electrode negatives to create the leg seat pockets in the leg holders. This photo shows four electrodes 0.9 mm wide by 0.5 mm thick after a single use.

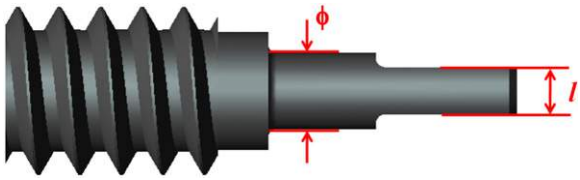

Figure 15. Drawing of the lead screw tip that interfaces with the gear. $\phi = 0.45$ mm and $l = 0.28$ mm.

a smooth cylindrical profile was created to interface with a bushing at the centre of the capsule. On the other end, the profile shown in figure 15 was created to enable it to interface with the larger central gear that can be seen in figure 2.

3.5.2. Fabrication strategy. The lead screw began as a commercial threaded rod (ISO M1 with a triangular profile). The primary considerations in choosing this profile were size and cost—it is useful to choose a small standard screw size so that a commercial tap can be used to thread the nuts. The threads were removed on short sections near the end of the lead screw. Thus, the primary fabrication challenge was shaping the end geometry shown in figure 15. This geometry is composed of two profiles, namely a $\phi = 0.45$ mm cylindrical region and a flattened tab 0.28 mm thick, which is inserted into the gear. A relatively large clearance (0.05 mm) is used at the screw–gear interface, making the assembly less sensitive to small positioning errors between the body and the caps.

We first attempted to fabricate the profile shown in figure 15 using the HSPC KERN. However, this method caused plastic deformation of the screw tip, so we opted for wire EDM.

3.6. The gears

3.6.1. Description. A gear transmission is included between the lead screw and motor to transmit and amplify torque from the motor to the lead screw. Gears with 17 and 40 teeth were fabricated to create this transmission. The smaller gear was attached to the motor shaft through the hole shown in

Figure 16. The brass gear. The design value for the addendum radius is 1.140 mm.

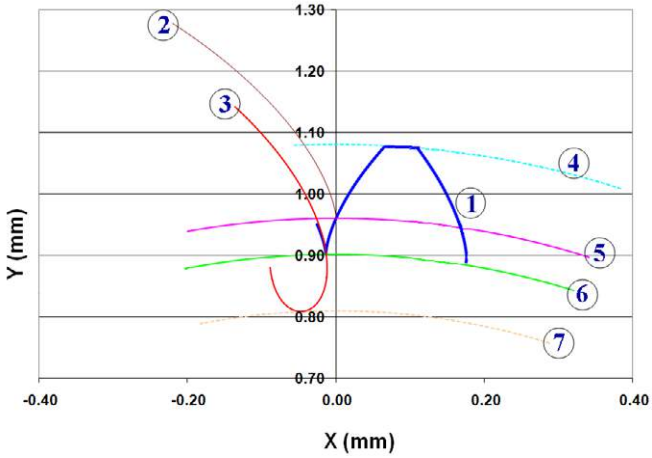

Figure 17. Shown above are curves taken from the output of the spreadsheet software that were used to define the gear tooth shape: (1) tooth profile, (2) evolvent curve; (3) profile of the curve easing; (4) addendum circle; (5) pitch circle; (6) base circle; (7) root circle.

figure 16. Since the fabrication method for both sizes of gear was the same, we discuss only the smaller gear in detail below.

3.6.2. Fabrication strategy. The traditional approach to toothed gear fabrication takes advantage of dedicated tools, based on standard modules. However, due to the stringent size requirements associated with fitting the entire mechanism in the available space inside the capsule, we required gears with modules smaller than those commercially available. One possible solution to this is to construct a customized tool for gear fabrication. However, this would have substantially increased the time and cost of the fabrication process.

Thus, we chose to use wire EDM to directly fabricate the gears. We believe that this approach is most useful for small quantities of custom module gears. When large quantities of identical gears are required, we suggest fabrication of a dedicated gear cutting tool for use on a gear cutting machine to achieve the desired module.

A brass plate was first machined using the HSPC KERN to create a round central hole. This hole was then enlarged and shaped as shown in figure 16 using the wire EDM. This particular quasi-rectangular shape was required to insert the motor shaft into the hole. We chose a custom module of 0.12 mm, which is a trade-off between the gear dimension constraints and ease of fabrication.

The wire EDM machine requires as input the Cartesian coordinates of sufficiently closely spaced points on the gear profile. We began with the characteristic parameters of the toothed gears (the module m and the number of teeth z). Then, applying standard gear theory [25], we developed a spreadsheet-driven software program that generated the coordinates of the profile points (figure 17). Finally, these data were exported in a file that was compatible with the machine.

As regards tolerance, a maximum deviation of -5 μm from the gear parameters' nominal values was adopted in order to obtain a correct assembly among the gear and the other components of the mechanism. This tolerance would allow for an acceptable clearance, thus guaranteeing proper operation of the device.

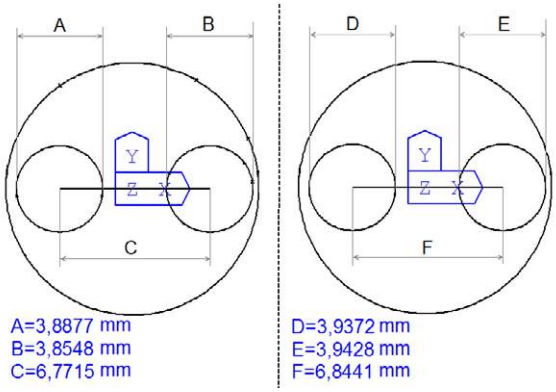

Figure 18. Measurement data from the VideoCheck machine. The cap (left) and the cap fixture (right).

4. Characterization and measurements

After manufacturing each of the components of the capsule robot as described in section 3 above, we conducted a series of measurements to evaluate the errors on specific features that are important to the overall function of the capsule robot. In particular, we used a digital optical microscope (MX-5040 RZ, Hirox, USA) and a Multisensor coordinate measurement machine (Benchtop VideoCheck® EA 400, Werth, Germany). In this section, we describe the results of these validation experiments.

4.1. The cap

Using the VideoCheck, we measured both the cap and the cap fixture described in section 3.1 (figure 18).

The measured value of interference is

$$\text{In} = \left(C - \frac{A+B}{2}\right) - \left(F - \frac{D+E}{2}\right) = -0.0039 \text{ mm}.$$

This interference enabled an accurate axial positioning and rigid fixturing (when combined with glue, as described in section 3.1) of the cap on the fixture.

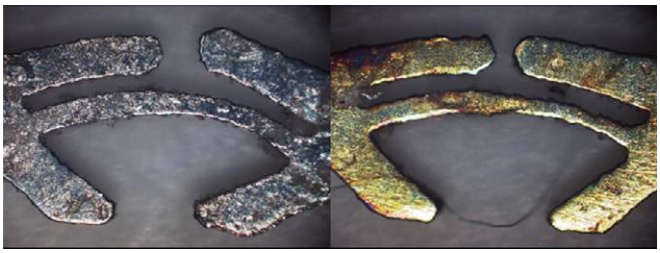

Figure 19. Two leg flexure joints machined with different techniques: (left) wire EDM; (right) laser cutting.

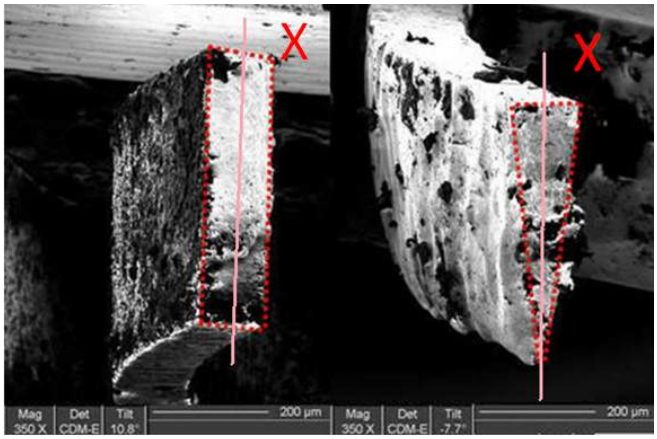

Figure 20. Cross-sections of knee flexure joints manufactured, using (left) wire EDM, and (right) laser cutting.

4.2. The leg

We measured the knee associated with the leg design shown in figure 10, because it is the most critical part regarding manufacture. In particular, we compared the quality of wire EDM and laser cutting techniques. A first evaluation was made by optical microscope as shown in figure 19.

The two legs were then imaged using a focused ion beam (FIB) microscope (200 THP, FEI, USA) and figure 20 shows cross sections of the knee. The leg cut by wire EDM has a rectangular cross-section as planned, while the cross-section of the laser cut knee is triangular. The knee can be modelled as a beam subject to bending; thus, according to elementary beam theory, the relationship between the applied bending moment M and the curvature κ of the beam is

$$\kappa = \frac{M}{EI}, \tag{1}$$

where E is the elastic modulus of the material and I is the cross-sectional inertia of the beam. Thus, all material properties and moments being equal, a beam with a triangular profile of a given height will have 1/3 the flexural rigidity (EI) of a rectangular beam of the same height (see figure 20). This reduction in rigidity is not acceptable for the devised application.

4.3. The leg holder

We measured the length and the width of the pin guide, the diameter of the pin hole where the leg holder connects to the nut and the dimensions of the leg seat. These measurements were repeated for six leg holders. In figure 21, one example of the measurements is shown and all the results are summarized in table 1.

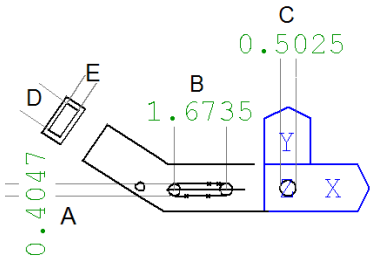

Figure 21. Measurement results of the leg holder.

Table 1. Measurement results for the leg holder.

	Design value (mm)	Average value (mm)	Minimum value (mm)	Maximum value (mm)	Standard deviation (mm)
A	0.4	0.406	0.403	0.408	0.0015
B	1.7	1.717	1.641	1.809	0.058
C	0.5	0.504	0.501	0.507	0.002
D	0.9	0.921	0.911	0.934	0.008
E	0.5	0.523	0.511	0.538	0.009

The hole for the pin (C) and the width of the guide (A) were machined with a good precision and repeatability. The variability in the length of the guide does not affect either the assembly or the functioning of the robot; in fact, the guide was purposely cut long enough that the pin never reaches either end of the slot. The measured values for the leg seat present some errors, but this is not a problem thanks to the elasticity of the leg junction.

4.4. The lead screw

The machined tip of the lead screw, where it connects with the gear (see figure 15), was observed by the optical microscope and the value of ϕ was calculated to be 0.452 mm, compared with a design value of 0.450 mm. It has to fit a bushing of 0.455 mm in diameter. With regard to l, we measured 0.270 mm, compared with a planned value of 0.280 mm, in order to fit a 0.29 mm hole in the big toothed gear.

The clearance between the flattened tab and the gear is an important part of the design because it allows easy assembly of the components and reduces the risk of damaging the screw.

An example optical microscope image of the lead screw tip is shown in figure 22.

4.5. The gears

To verify the manufacture quality for the small gear, dimensional control was carried out with the VideoCheck system mentioned earlier. From the measurement system, we obtained the coordinates of points along the gear profile (figure 23). These data were used to calculate the actual gear parameters, which were compared with the design parameters for the gear (table 2).

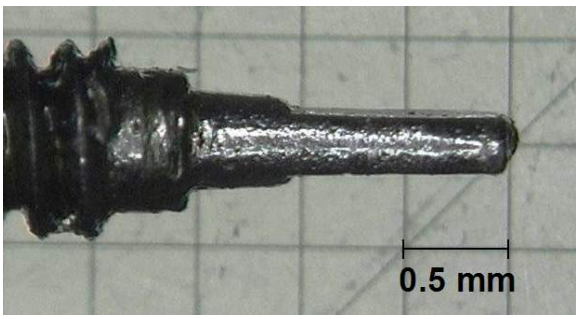

Figure 22. Optical microscope image of the lead screw tip.

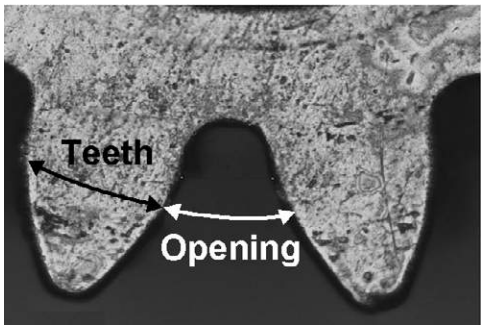

Figure 23. Picture of the tooth profile taken by the VideoCheck machine.

Table 2. Data for the toothed gear. Half-pitch of openings and teeth. Statistical data are obtained considering all the teeth of the gear

	Design (mm)	Average (mm)	Max. (mm)	Min. (mm)	SD
Opening	0.1884	0.20	0.23	0.19	0.02
Teeth	0.1884	0.17	0.20	0.16	0.01

First we note that the gear profile is not perfectly centred with the gear rotation axis. This is probably due to switching the part from the HSPC KERN to the wire EDM. Second, the teeth are slightly smaller than their intended dimensions. This was related to the wire EDM fabrication and could be compensated for by adjusting the profile by the wire and arc dimensions. However, for our purposes it is preferable for gears to be slightly undersized rather than slightly oversized, since undersized gears can mesh with one another. We also note that these gears functioned well in our prototype at the dimensions given in table 2.

5. Assembly process

Assembling all the small parts in a meso-scale robot is a challenging operation requiring close attention to avoid damaging components during assembly. Figure 24 presents an exploded view of the capsule, illustrating how the parts fit together.

The general procedure for assembling the capsule is as follows. Starting with the capsule body, the motors were inserted and held in place with glue. Next, the bushings were inserted. Then the subassembly of the nut and leg holders

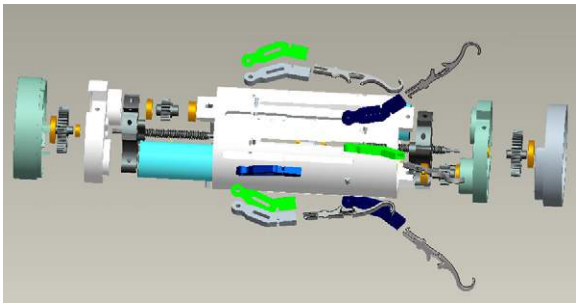

Figure 24. Exploded view of the capsule robot.

was separately assembled and inserted into each end of the capsule. In the next step, the two lead screws were inserted in each nut. The caps and gears were then assembled on each end, followed by snapping one leg into each leg holder using the flexure attachment visible in figure 10 at the base of the leg.

One assembly challenge was the insertion of the nut and leg holders into the capsule body, due to the narrow space between the components. Another was in attaching the gear to the screw: care was necessary to prevent breaking the very thin screw tip. An additional challenge was inserting the motor into the body before the glue dried, fixing it in place.

These challenges led to some broken components during initial assembly. Furthermore, care was necessary to keep the mechanism clean and free of dirt and chips from the fabrication process. With respect to parts fixed by glue, the main challenge was to apply the correct amount of glue. Excessive glue would spread to unintended locations, while an insufficient amount of glue would dry too rapidly to allow components to seat properly. Fortunately, it was possible to remove the glue with a solvent, enabling the correct amount to be determined via trial and error. None of these assembly challenges was insurmountable—the assembled capsule functioned very well in comparison to overall design objectives regarding foot forces and ranges of motion—see [26] for details on these issues.

6. Discussion and conclusion

The fabrication of a centimetre-size robot, with most components in the meso-scale domain, was presented in this paper as a case study on the use of multiple precision machining technologies and refixturing processes to create meso-scale components that can be assembled into complex mechanisms. Many of the components created have complex 3D shapes and also present features in the micro-scale.

The single parts and their dimensional features are summarized in table 3, together with the manufacturing techniques used to fabricate them, the advantages/disadvantages of the selected solutions and the average dimensional errors of the finished components. From the table one can observe that the most complex parts required the synergetic use of several different precision machining techniques. One of the main challenges in this case is

Table 3. Single parts and their dimensional features, manufacturing techniques adopted, advantages/disadvantages of the selected solution and average dimensional errors of the finished components.

Capsule part	Dimensional features	Manufacturing techniques	Advantages/disadvantages	Fabrication errors
Cap	$\Phi = 11.1$ mm; smallest features: several 150 μm thick regions	Two HSCP KERN processes, one per side	−Particular care was required for part refixturing	28 μm error in 6.8 mm inter-axis spacing
Body	$\Phi = 11.1$ mm; $l = 23.6$ mm; smallest features: 12 holes of 0.4 mm diameter around the external surface	Two HSCP KERN processes, one per side	−Particular care was required for part refixturing; −Drilling lateral holes on the external surface required a surface levelling procedure.	N/A—no features in the body required exceptionally high tolerances for overall device function
Leg	$l = 9.4$ mm; smallest features: 0.075 mm thick flexible knee. 0.1 mm hooks	Wire EDM	+ Rectangular profile; −Rougher surface than laser	N/A—legs functioned according to design objectives
Leg	$l = 9.4$ mm; smallest features: 0.075 mm wide flexible knee	Laser cutting	+ Faster than Wire EDM; −Triangular profile	Material erosion impaired correct knee shaping
Leg holder	$l = 7.38$ mm; smallest features: 0.4 mm wide pin guide	Wire EDM, Sink EDM; The Sink EDM electrode required HSPC KERN and Wire EDM	−3 Sink EDM electrodes are required to machine 1 leg-holder	8 μm error in 0.4 mm pin guide width; 7 μm error for the 0.5 mm hole
Lead screw	Relevant features: $\phi =$ 0.45 mm; $l = 0.28$ mm	Wire EDM	+ Plastic deformation was avoided thanks to the selected fabrication process	2 μm on ϕ; 10 μm on l
Gears	Addendum radius = 1.140 mm; module = 0.12 mm	HSPC KERN and Wire EDM	+ This procedure enabled completely customizable gear modules; −A purposely developed spreadsheet was required to input the Cartesian coordinates to the Wire EDM	41 μm error for the 0.1884 mm half pitch

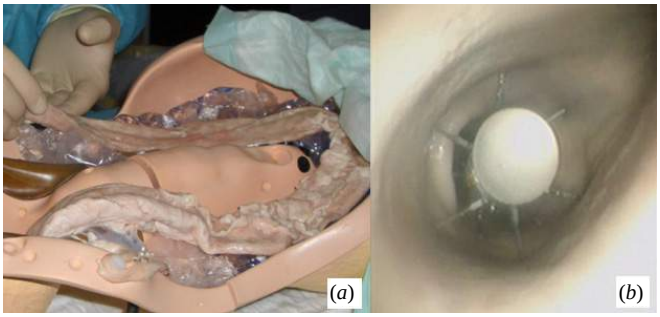

Figure 25. The capsule moving in a porcine colon. (*a*) External view in a phantom model and (*b*) endoscopic view.

maintaining accurate references when moving a part between machines or refixturing it on a given machine.

After fabrication, several measurement techniques were used to characterize individual parts and compare them to the original design intent. The final test in whether manufacturing accuracy was sufficient was assembly of the capsule and verification of its function. We were able to successfully assemble the 72 parts into a working capsule robot that successfully utilized legged locomotion to travel through the porcine colon (see [26, 27] as well as figure 25).

In initial tests the capsule achieved a maximum speed of 50 mm min^{-1}, which is suitable for performing an entire colonoscopy in a length of time consistent with conventional colonoscopy. The capsule prototype is also able to climb in any direction—including vertically against gravity.

The results presented in this paper on capsule component manufacture and assembly illustrate the unique challenges intrinsic to the meso-scale. Perhaps more importantly, they also provide examples of solutions to meso-scale manufacturing challenges. We believe that the combination of these results with those of other researchers will strengthen the emerging framework of best practices in meso-scale design, manufacture and assembly. This will lay the foundation for many innovative future devices.

Acknowledgments

This material is based in part upon work supported by the Intelligent Microsystem Center, KIST, South Korea, in part by the European Commission in the framework of VECTOR FP6 European Project EU/IST-2006-033970, as well as the National Science Foundation GRFP.

The authors would like to thank Novineon Healthcare Technology Partners GmbH, in Tübingen (Germany), for assistance during the testing phase of the device. The magnetic encoder was developed by Sensitec GmbH and laser cutting of the legs was performed by Endosmart GmbH within the

framework of the VECTOR European Project. The authors are also grateful to N Funaro, C Filippeschi and G Favati for prototype manufacture, as well as M Quirini and C Stefanini for their invaluable technical support.

References

[1] Receveur R A M, Lindemans F W and de Rooij N F 2007 Microsystem technologies for implantable applications *J. Micromech. Microeng.* **17** R50–80
[2] Fujimasa I 1996 *Micromachines: A New Era in Mechanical Engineering* (New York: Oxford University Press)
[3] http://www.givenimaging.com
[4] Suryaprakash M V 2004 *Precision Engineering* (Oxford: Alpha Science International)
[5] Madou M J 2002 *Fundamentals of Microfabrication: The Science of Miniaturization* (Boca Raton, FL: CRC Press)
[6] Cheng Y and Lai J 2008 Fabrication of meso-scale underwater vehicle components by rapid prototyping process *J. Mater. Process. Technol.* **201** 640–4
[7] Cham J G, Bailey S A, Clark J E, Full R J and Cutkosky M R 2002 Fast and robust: hexapedal robots via shape deposition manufacturing *Int. J. Robot. Res.* **21** 869–82
[8] Vogler M P, Liu X, Kapoor S G, DeVor R E and Ehmann K F 2002 Development of meso-scale machine tool (mMT) systems *Trans. NAMRI/SME* **30** 653–61
[9] Kim Y T, Park S J and Lee S J 2005 Micro/meso-scale shapes machining by micro EDM process *Int. J. Precis. Eng. Manuf.* **6** 5–11
[10] Chae J and Park S S 2007 High frequency bandwidth measurements of micro cutting forces *Int. J. Mach. Tools Manuf.* **47** 1433–41
[11] Okazaki Y, Mishima N and Ashida K 2002 Microfactory and micro machine tools *1st Korea Japan Conf. Positioning Technol.* pp 150–5
[12] Eisinberg A, Menciassi A, Dario P, Seyfried J, Estana R and Woern H 2006 Teleoperated assembly of a micro-lens system by means of a micro-manipulation workstation *Assem. Autom.* **27** 123–33
[13] Chae J, Park S S and Freiheit T 2006 Investigation of micro-cutting operations *Int. J. Mach. Tools Manuf.* **46** 313–32
[14] Dornfeld D A 2006 Recent advances in mechanical micromachining *Ann. CIRP* **55** 2
[15] Yu Y Z 1998 Micro-EDM for three-dimensional cavities—development of the uniform wear method *Ann. CIRP* **47** 1
[16] Rajurkar K P 2000 3D Micro-EDM using CAD/CAM *Ann. CIRP* **49** 1
[17] Iddan G, Meron G, Glukhovsky A and Swain P 2000 Wireless capsule endoscopy *Nature* **405** 417
[18] Waterman M and Eliakim R 2008 Capsule enteroscopy of the small intestine *Abdom. Imag.* **34** 452–8
[19] Park H, Park S, Yoon E, Kim B, Park J and Park S 2007 Paddling based microrobot for capsule endoscopes *IEEE Int. Conf. on Robotics and Automation* pp 3377–82
[20] Dario P, Ciarletta P, Menciassi A and Kim B 2004 Modeling and experimental validation of the locomotion of endoscopic robots in the colon *Int. J. Robot. Res.* **23** 549–56
[21] Quirini M, Menciassi A, Scapellato S, Stefanini C and Dario P 2008 Design and fabrication of a motor legged capsule for the active exploration of the gastrointestinal tract *IEEE-ASME Trans. Mechatronics* **13** 169–79
[22] Quirini M, Menciassi A, Scapellato S, Dario P, Rieber F, Ho C N, Schostek S and Schurr M O 2008 Feasibility proof of a legged locomotion capsule for the GI tract *Gastrointest. Endosc.* **67** 1153–8
[23] Quirini M, Webster R J III, Menciassi A and Dario P 2007 Design of a pill-sized 12-legged endoscopic capsule robot *IEEE Int. Conf. on Robotics and Automation* pp 1856–62
[24] Buselli E, Valdastri P, Quirini M, Menciassi A and Dario P 2009 Superelastic leg design optimization for an endoscopic capsule with active locomotion *Smart Mater. Struct.* **18** 015001
[25] Childs R 2003 *Mechanical Design* (London: Butterworth-Heinemann) chapter 6
[26] Valdastri P, Webster R J III, Quaglia C, Quirini M, Menciassi A and Dario P 2009 A new mechanism for meso-scale legged locomotion in compliant tubular environments *IEEE Trans. on Robot.* at press (doi:10.1109/TRO.2009.2014127)
[27] Menciassi A, Valdastri P, Harada K and Dario P 2008 Single and multiple robotic capsules for endoluminal diagnosis and surgery *IEEE/RAS-EMBS Int. Conf. on Biomedical Robotics and Biomechatronics* pp 238–43